

THE BEAM BREAKUP INSTABILITY IN PULSED TRANSMISSION LINE LINEAR ACCELERATORS^{a)}

R. J. Adler^{b)}, T. C. Genoni^{c)}, and R. B. Miller^{d)}

Abstract

The transverse Beam Breakup Instability (BBI) can result in reduced pulse length in linear accelerators. A brief summary of the instability mechanism and a gain formula are presented. Test bench measurements of the two relevant parameters, transverse shunt impedance Z_{\perp} , and cavity Q have been made. These measurements illustrate the importance of transmission line dielectric and cavity geometry to the gain. Results indicate that Q may vary from 10 - 75, and that Z_{\perp}/Q is in the range 4 - 70 Ω .

Introduction

The Beam Breakup Instability (BBI) was originally observed on the SLAC accelerator,^{1,2} and may be a limiting factor in the construction of the new generation of high current linear accelerators.³⁻⁵ Previous work has centered on instability theory,^{2,6,7} and cavity measurements in ferrites⁸ or iron core linacs.⁹ In the first section of this paper, instability theory is reviewed including the effects of the spatial phase of the initial and perturbed transverse momenta. In the second section, the results of a series of 'testbench' measurements on typical radial transmission line accelerating cavities are summarized. Finally, the measured quantities are applied to theory in the third section.

Instability Theory

The instability results from the coupling between a beam oscillating off-axis, and accelerating cavity modes with a transverse magnetic field on axis (TM₁₀ modes, for example). The accelerating cavities are assumed to be identical, with identical resonant frequencies, and the cavities are assumed to be coupled only by the beam oscillation. Let ξ be the transverse displacement of the beam centroid at the TM₁₀ resonant frequency $\xi = \xi_0 \sin \omega t$. A beam entering an accelerating cavity is equivalent to an oscillating dipole loop of current $2IM\xi_0/r\pi$ where I is the total beam current, r is the beam radius, $M = (\sin \omega\ell/2c)/(\omega\ell/2c)$ is the modulation coefficient defined by Siambis,⁷ ℓ is the length of the accelerating gap, and c is the assumed velocity of the relativistic beam (the speed of light). Assuming that the phase shifts of the centroid between cavities are fixed in time, cavity mode energy will build up, and will be in temporal phase with the centroid (i.e., $B_{\perp} \propto \xi$ for all cavities). If the initial perturbation amplitude is fixed or decreasing in time, the instability will grow to its maximum in one cavity energy storage time, $\tau > Q/2\omega$ where Q is the usual cavity quality factor. In steady state the change in transverse momentum in the nth cavity $\delta p_{\perp n}$ is related to the centroid displacement entering the nth cavity, ξ_n by

$$\delta p_{\perp n} = m \left(\frac{Z_{\perp} I}{510} \right) \omega \xi_n \quad (1)$$

where I is in units of kiloamps, and Z_{\perp} (ohms) is defined as⁶

$$Z_{\perp} = \frac{Q \left[\int_0^{\ell} B_{\perp} dz \right]^2}{2\omega U} c^2 \quad (2)$$

where U is the cavity stored energy.

Note that $\delta p_{\perp n}$ is in the same direction as ξ , however, $p_{\perp n}$ is not, in general, in the same direction as ξ . The details of adding $p_{\perp n}$ and $\delta p_{\perp n}$ are time dependent, and also depend on the polarization of the cyclotron wave that ξ represents.

In general, we know that vector addition gives $p_{\perp n+1} < p_{\perp n} + \delta p_{\perp n}$. A useful lower limit to the addition is given by the circularly polarized cyclotron mode as $p_{\perp n+1} \geq (p_{\perp n}^2 + \delta p_{\perp n}^2)^{1/2}$. Noting that in general, for cyclotron motions we have $\xi_n = p_{\perp n}/m\gamma\omega_c$, the gain $G = p_{\perp n+1}/p_{\perp n}$ of the instability is found from equation (1) as

$$(1 + G_f^2)^{1/2} < G < 1 + G_f$$

$$G_f = \frac{Z_{\perp} I \omega M^2}{510 \gamma \omega_c}$$

The recent numerical work performed by one of the authors (TCG, to be published) indicates that for $G_f < 1$, G is approximately half way between the two bounds, but approaches the lower bound for $G_f > 2$. The upper bound on G is equivalent to equations 5.13 and 5.14 of reference 6, while G_f is similar to the factor G defined by Siambis.⁷ It is important to note that the instability always grows, apart from phase mixing, and that $G_f < 1$ does not result in stability, contrary to reference 7.

Testbench Measurements

A typical cavity (diode) for a linear accelerator driven by pulsed transmission lines is shown in Fig. 1. The grading rings act as a high voltage standoff and dielectric-vacuum interface, while the fieldshapers shorten the accelerating gap and minimize E_r . The diode of Fig. 1 was designed for ~2 MV.

As a microwave problem, the diode is complicated since it is not a simple shape (a re-entrant cylinder), and the grading rings form a complicated boundary surface. An effort was made to separate the various effects in the measurements. Table 1 lists the cavity Q in a variety of configurations.

A comparison of examples A and F indicates that the grading ring cavity is lossy compared to a metal-walled cavity. At frequencies above 2 - 3 GHz, the Q of modes in configuration C drop to <40, indicating that TM10 will be the important beam breakup mode in pulsed transmission lines. The fieldshapers tend to increase the cavity Q in the grading ring structure as evident from A - C. Measurements with electric field probes outside the grading rings indicate that the fields extend beyond the rings. This is significant when using high- ϵ dielectrics which have significant losses above 500 MHz, such as water or ethylene glycol. Case D

a) This work was supported by the Air Force Weapons Laboratory and Sandia National Laboratories.
 b) Mission Research Corporation, 1400 San Mateo Blvd., S.E., Suite A, Albuquerque, New Mexico 87108.
 c) Air Force Weapons Laboratory, Kirtland Air Force Base, New Mexico 87117.
 d) Sandia National Laboratories, Albuquerque, New Mexico 87185.

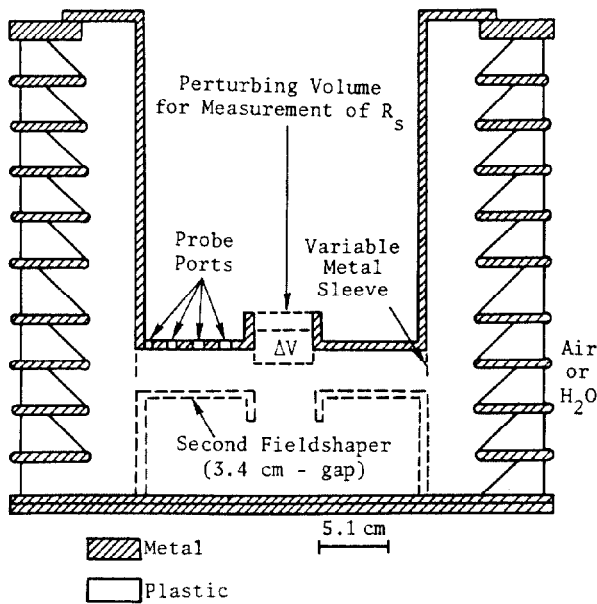


Figure 1. Typical grading ring diode cavity.³ The dashed lines indicate the optional movable sleeve, optional second fieldshaper for the 3 - 4 cm gap, and the perturbing volume.

Table 1
Summary of Cavity Q Measurements
in Various Configurations.

GEOMETRY	OUTER DIELECTRIC	DRIFT PIPE	f Ghz	Q
A Cylindrical No Fieldshaper	air	----	1.31	35
B A + upper Fieldshaper	air	open	1.92	50
		closed	1.92	73
C A + two Fieldshapers	air	open	1.85	77
		closed	1.85	70
D A + upper Fieldshaper	H ₂ O	open	1.55	10
E A + two Fieldshapers	metal walled	open	1.86	105
F A	metal walled	----	1.38	460

indicates that Q is substantially reduced when water, the dielectric of choice for high energy density accelerators, is used.

The effect of the cavity shape is evident from comparing E and F in Table 1. The frequency increases ~30 - 40% due to the fieldshaper. This is also evident from the measured and theoretical data in Fig. 2. The electric field profile peaks near the center of the fieldshaper rather than the $J_1(x = r/R)$ electric field dependence shown by the dashed line. The solid line is a numerical solution to the problem and is similar to a combination of TM 110 and 111 modes of the H-shaped cavity shown in Fig. 2. The mode frequency is dominated by the fieldshaper dimension, at least in this example.

The measurements of the second unknown, Z_1/Q , was accomplished by using the method of Hansen and Post.¹⁰

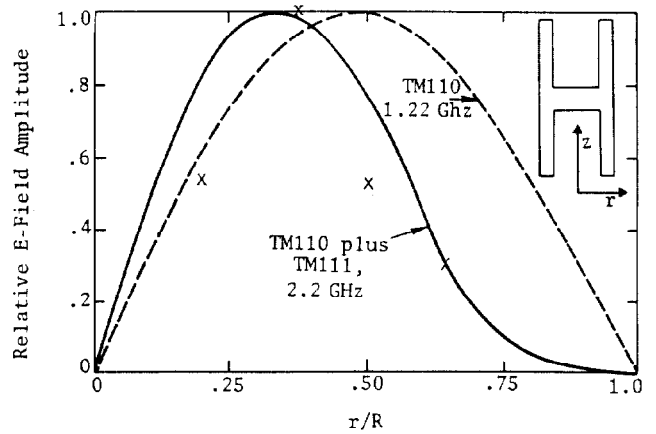


Figure 2. Axial electric field as a function of radius for case B. The X's are experimentally measured points, the dashed line is the theoretical value for a cylindrical cavity, and the solid line is the numerical solution for the H-shaped cavity shown in the upper right corner.

The penetration depth of the small volume ΔV , shown in Fig. 1, was changed in a quasi-continuous fashion, and the frequency shift was noted. Several examples of such curves are shown in Fig. 3. Using the Slater perturbation theorem,¹¹ assuming that B_1 is uniform near the perturbing volume, and noting that $E_z = r\omega B_1$, we have for TM110-like modes

$$\frac{Z_1}{Q} = \frac{2c^2 \mu_0 \ell^2}{\left[1 - \left(\frac{r\omega}{2c}\right)^2\right] \omega} \left(\frac{1}{\omega} \frac{d\omega}{dV}\right) \quad (4)$$

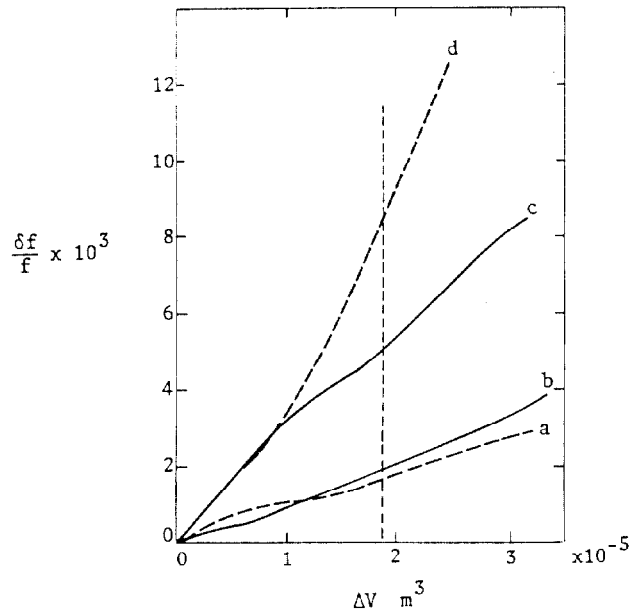


Figure 3. Transverse impedance measurement curves of $\delta E/E$ as a function of δV for a) no metal sleeve, b) 1.27 cm sleeve extension, c) 2.54 cm sleeve extension, and d) full sleeve extension which is equivalent to a right circular cylinder. The dashed line corresponds to an unperturbed cavity.

where r is now the radius of the perturbing volume. The method above was verified by measuring Z_1/Q for cylindrical cavities with $R = 10.2$ cm, and $l = 3.4$ or 8.9 cm. The values were then compared with the theoretical value of $96 l/R \Omega$ computed from equation (2). The agreement found was $\sim \pm 30\%$. Impedance measurements for several configurations are given in Table 2.

Table 2

Various Transverse Impedance Measurements.
One drift tube is open in all $l = 3.5$ cm measurements.

CAVITY CONFIGURATION	R (cm)	l (cm)	f (Ghz)	Z_1/Q
Pill Box	10.2	3.5	1.68	20
	10.2	8.9	1.77	106
Open Rings		8.9	2.54	11
		8.9	1.93	72
		3.5	1.89	4
Metal Liner replacing rings		8.9	2.30	42
		3.5	1.90	4

Table 2 indicates that the impedance of the cylinder is much higher than that of the diode. The metal sleeve measurements of Fig. 3 demonstrate the transition from the cylinder(d) to diode(a) cases. In effect the coupling to the outer part of the diode increases as the sleeve is retracted, so that for fixed B_z , U (cavity field energy) increases. For the smaller gap, U is dominated by the field contribution from outside of the fieldshaper.

For the 3.5 cm gap, $\sim 80\%$ of the-field energy is outside a gap, while $\sim 50\%$ is outside the gap for the 8.9 cm case.

Conclusion

Given the data of the previous section and equation (3), we may estimate the instability gain in a pulsed transmission line Linac using a water dielectric. Sample parameters and gains are shown in Table 3 for a Q of 10. The values of Z_1/Q are interpolated from Table 2.

Table 3

Instability Gains for a Cavity Frequency of 2 Ghz, based on Equation 3 and Table 2

I kA	l cm	Z_1/Ω	B_z kG	$1 + G_F$	$(1 + G_F^2)^{1/2}$
50	6	200	15	1.56	1.15
100	6	200	15	2.12	1.50
100	6	200	20	1.84	1.30
100	5	120	15	1.76	1.26
100	3.5	40	15	1.31	1.05
10	2.5	20	5	1.05	1.0012

As can be seen from Table 3, for 100 kA, large gains ($>10^4$ for 15 stages) can result, however, the gain is quite acceptable at 50 kA for 10 rather than 15 stages. Preliminary results indicate that if necessary, minor cavity modifications (increasing the fieldshaper diameter, for example) can change the resonant frequency up to $\pm 15\%$. In this way taking a 30 stage accelerator with cavities at 3 different frequencies, gains could be reduced to less than 100.

References

1. R. Helm and G. Loew, "Beam Breakup," Chapter B.1.4 in Linear Accelerators, P. M. Lapostolle and A. L. Septier, North Holland, Amsterdam.
2. W. Panofsky and M. Bander, "Asymptotic Theory of Beam Breakup in Linear Accelerators," Rev. Sci. Inst. 39, 2076 (1968).
3. R. B. Miller, et al, "Multistage Linear Electron Acceleration Using Pulsed Transmission Lines," to be published in Journal of Applied Physics.
4. A. C. Paul, et al, "Characteristics of the ETA Gun," Lawrence Livermore Report UCRL-84065, (1980).
5. A. I. Pavlovsky, et al, "Multielement Accelerators Based on Radial Lines," Sov. Phys. Dokl. 20, 441 (1980).
6. V. K. Neil, L. S. Hall, and R. K. Cooper, "Further Theoretical Studies of the Beam Breakup Instability," Part. Accel. 9, 213 (1979).
7. J. G. Siambis "m=1 Cyclotron Mode Klystron Instability," Phys. Rev. Lett. 42, 1677 (1979).
8. D. L. Birx, "Microwave Measurements of the ETA Accelerating Cavity," UCID-18582 (1980).
9. "Resonance Q Investigation and Beam Instability Studies of a High Current Induction Linac," Haimson Res. Corp., Rept. HRC-703, Burlington, Mass., 1972.
10. W. W. Hansen and R. F. Post, "On the Measurement of Cavity Impedance," J. Appl. Phys. 19, 1059 (1948).
11. J. C. Slater, Microwave Electronics (D. Van Nostrand Co. Inc., New York, 1950) p. 81.